5.3.4. Optimization

In calculating the simulated counts, C_{ij}, the gain factor, G and the dead-time, τ, are known only approximately. Also, the effective attenuation coefficient through the reactor medium depends on the local gas hold-up profile (representative of distribution of the reactor media density, which is unknown). Thus, one has to resort to an optimization technique to get the optimal values of G, τ and the three parameters in the universal gas hold-up profile

$$\varepsilon_g(\zeta) = \tilde{\varepsilon}_g\left(\frac{m+2}{m}\right)\left(1-c\zeta^m\right)$$
$$\bar{\varepsilon}_g = \tilde{\varepsilon}_g\left(\frac{m+2-2c}{m}\right)$$

Although the holdup profile in two-phase bubble columns is known to deviate from the form proposed above (generally, true only in the well developed section of the column), the variations with the reactor axis are not known to be significant except near the distributor and disengagement zones. As the variations in these zones are not well quantified and modeled, for this work at the moment, the variation of the profile with the column axis has been neglected.

For each detector, the objective function, to be minimized, is defined as:

$$OBJ_i = \sum_{j=1}^{N_{cali}} W_{ij}\left(\frac{\left(C_{ij}-M_{ij}\right)}{\left(C_{ij}+M_{ij}\right)/2}\right)^2$$

$M_{ij} \equiv$ measured counts.

$C_{ij} \equiv$ simulated counts.

$W_{ii} = \dfrac{\sqrt{W_{ii}}}{\sum_{i=1}^{N_{cali}}\sqrt{W_{ii}}} \equiv$ weighting factor for detector i and calibration point j.

The following approximation in the evaluation of the photo-peak efficiency has been used for computational efficiency. When the results are compared to the case when no approximation is used, the errors rarely exceed 1%.

$$P_e = \iint_\Omega \frac{\vec{r}.\vec{n}}{r^3} f_a(a,q) f_p(a,q)\,ds \approx \iint_\Omega \frac{\vec{r}.\vec{n}}{r^3} f_p(a,q)\,ds \iint_\Omega \frac{\vec{r}.\vec{n}}{r^3} f_a(a,q)\,ds$$

The discretized form of the above integral becomes

$$P_\varepsilon \approx \frac{1}{4}\sum_{i=1}^{n}\sum_{j=1}^{n} w_g(i)w_g(j)w\left(\alpha_i,\theta_j\right) \times \frac{1}{4}\sum_{i=1}^{n}\sum_{j=1}^{n} w_g(i)w_g(j)w\left(\alpha_i,\theta_j\right)f_p\left(\alpha_i,\theta_j\right)f_a\left(\alpha_i,\theta_j\right)$$

The above optimization for our case is being implemented through a *generalized reduced gradient* method using the code GRG2. Once the optimization routines successfully converge to provide the optimal values of the optimized variables, a 3-D distance-count map is generated for each detector. The map could be created for as fine a resolution as desired, limited only by the finite size of the neutrally-buoyant radioactive flow follower, the statistical nature of the radiation, and constraints of computer memory and storage costs.

With the calibration map already available, an actual experiment is carried out in which a neutrally-buoyant tracer is let free in the flow, and the counts emitted by it are registered by each detector at finite time intervals (20 ms for a usual CARPT experiment). Programs have been developed to compute the chi-squared values of the measured counts against those from the calibration map. The location from the calibration map, which provides the minimum chi-squared value, is taken as a coarse estimation of the particle position at that instant of time. To get the exact particle position, a 3-D interpolation and minimization using Powell's routine are implemented on the chi-squared values of the 26 closest neighbors of the above point (the mathematical details are not being provided here). Thus, the particle location is accurately estimated by this procedure at every instant of time.

5.4. Theoretical Validation

The computer codes required for optimization, calculation of photo-peak efficiencies, and particle position reconstruction from dynamic counts data have been ***validated*** against theoretically simulated data. The details of the validation results are presented elsewhere (Gupta, 1997). The two important results from the simulations are

- The peak to total efficiency ratio is not a constant and is dependent on the location of the source with respect to the detector.
- Thirty point Gaussian quadrature in each direction during a surface integration, are sufficient to accurately simulate the photo-peak of each detector.

5.5. Experimental Validation

The ultimate test of the reliability of any numerical technique based on physical models is achieved when one validates the programs with real experimental data. As the Monte Carlo procedure systematically models the photo-peak fraction (or the counts associated with the photo-peak), it is necessary that while acquiring the counts during an experimental run, the thresholds and sampling windows are correctly set so as to sample just the photo-peak counts. This is best achieved by measuring the emitted energy spectrum from a point source using a Multi Channel Analyzer (MCA) so that the start and end of the photo-peak could easily be identified. Since Sc^{46} does not emit photons having energy above 1.2 MeV, the possibility of pair production is rare and therefore, one does not need to worry too much about the end of the photo-peak. The only thing one has to control though, is the threshold, or the start of the photo-peak, and adjust the hardware settings correctly so as to properly sample the requisite counts. Experimental data for verification of the Monte Carlo approach presented here was acquired in a cylindrical Plexiglas column with an i.d. of 7.47" and o.d. of 8.0". The schematic of the experimental setup and data acquisition is shown in Figure 5.4.

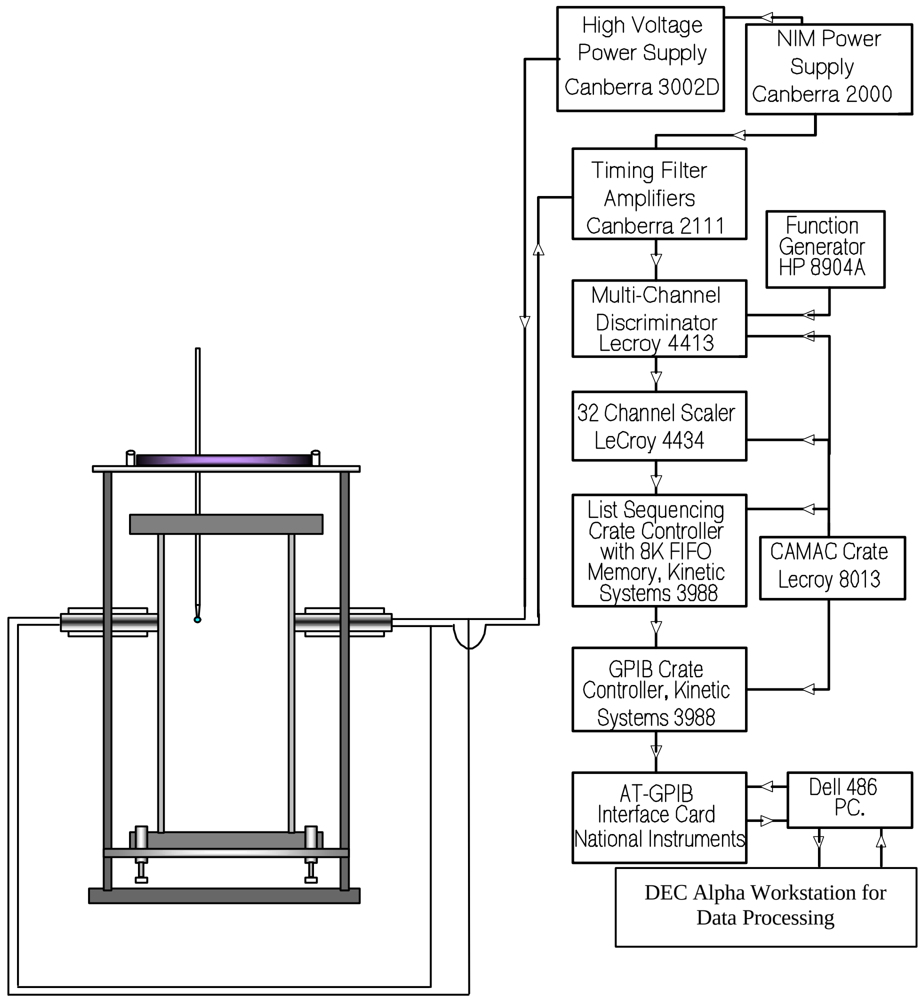

Figure 5.4: Schematic of the Experimental Setup to Verify the Monte Carlo Simulations

A set of four 2"x2" NaI(Tl) detectors was used for the data acquisition. The detectors were mounted flush to the column at an axial level of 35.4 cm from the bottom of the column. The detectors were positioned at 90^0 degrees to each other (in the plane of the detectors). The total column height used for the reported experiments was 48 cm. experiments were conducted with an empty column, the column filled with water, and with air being sparged into the column filled with water. The objectives of the experiments were twofold. Since the modeled counts belong only to the photopeak portion of the spectrum, the first objective was to determine the correct threshold for the data acquisition system. The second objective was to acquire data at this critical threshold to verify the optimization routines, and to evaluate the particle-position-reconstruction programs against such experimental data.

Figure 5.5 displays the results of the spectrum analysis for the four detectors used in this study. The radiation counts were acquired by placing the radioactive particle in the center of the column, in the plane of the detectors. It is clear from the figure that a threshold of 300 mV is appropriate as the one signifying the start of the photopeak portion of the spectrum. The Sc^{46} isotope has two photopeaks at 0.889 MeV and 1.12 MeV. Depending on the amplifier gain settings, different threshold scales (mV) map to the same scale of γ-ray photon energies.

The two photopeaks of the Sc^{46} isotope are evident from Figure 5.5. Similar analysis was carried out for other locations of the radioactive source. Though the Compton portion of the spectrum showed dependence on the location of the radioactive source, the photopeak portion of the spectrum was almost independent of the location of the source in terms of the start of the photopeaks. With an identified critical threshold of 300 mV, the data was acquired with the radioactive particle placed in 27 different locations, at a sampling frequency of 50 Hz for a total sampling time of 3.84 seconds. These 27 positions were located on 3 planes, one of the planes being the plane of the detectors, with another plane at above and one below of this plane. In each plane, the data was acquired with the particle placed at the center of the column, and at eight other positions located on a circle of radius 5 cm 45^0 apart. The source strength of the particle used in this study was approximately 95 μCi.

Figure 5.6 shows the comparison of the experimentally observed particle position to the one reconstructed by the procedure outlined above. The experiments were conducted with water as the intervening medium. A resolution of 1 cm was used for generating the 3-D grid over which the particle position is reconstructed. The position reconstruction in the x-y plane is satisfactory given the grid that was used. However, the resolution in the z-direction is far from satisfactory. Similar trends were observed in an empty column, as well as in the one with a gas-liquid dispersion. The reason for this observation is straightforward. A set of four detectors is used to resolve the particle position in the x-y plane, whereas only one level of detectors are used to resolve the particle position in the z-direction -- hence, the observed inaccuracy is inherent in this experimental design which was utilized only as a quick test of the proposed method. A full-scale data acquisition, with multiple detector-levels has to be accomplished to fully resolve the z-coordinate of the particle position. Nevertheless, these results validate the numerical technique, and further experimentation, along with modifications in the numerical schemes for particle position reconstruction are being evaluated to refine the procedure.

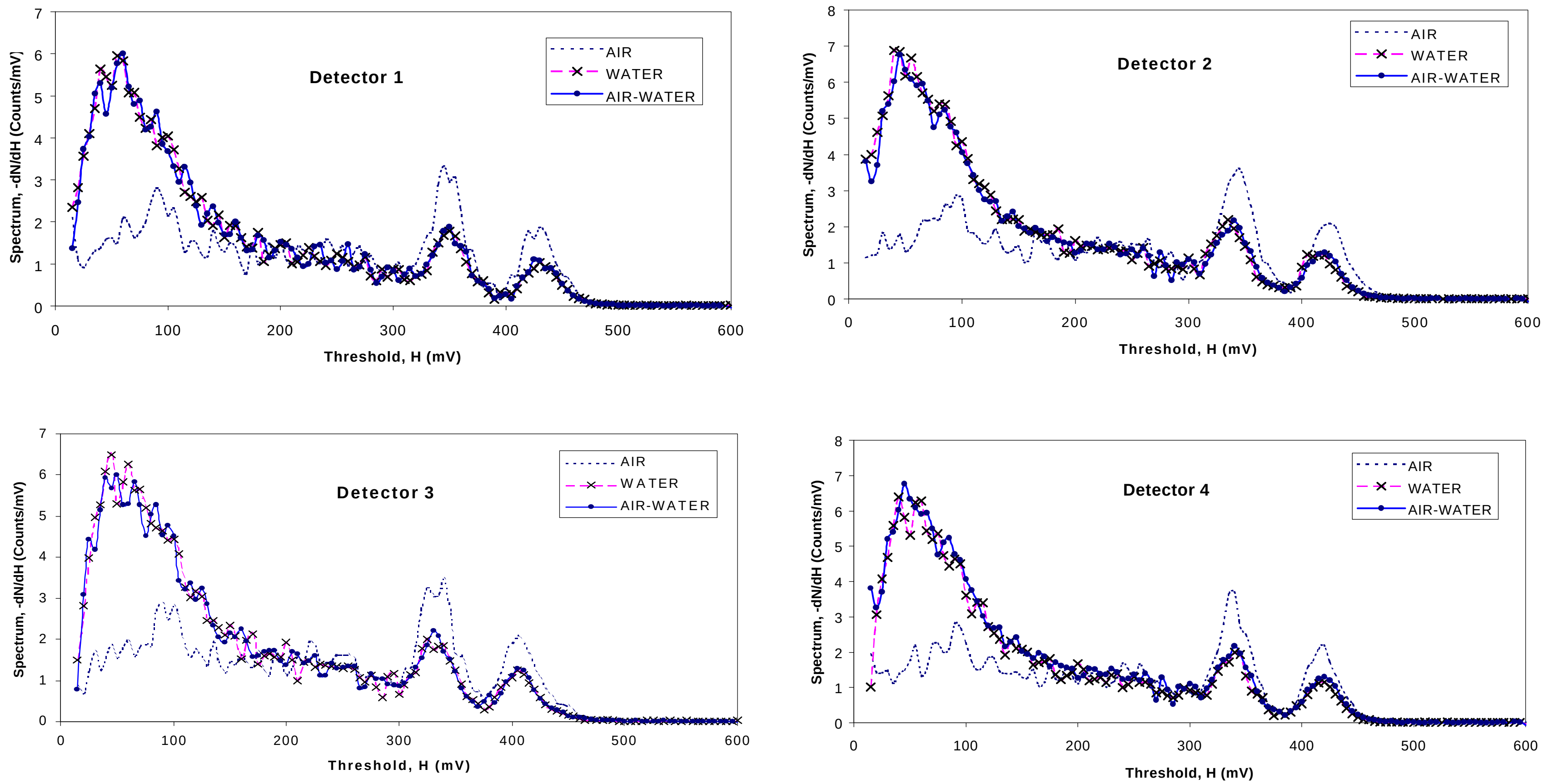

Figure 5.5: Spectrum Analysis of the Four Detectors used in the Experiments for Identification of the Threshold Signifying Beginning of the Photopeak

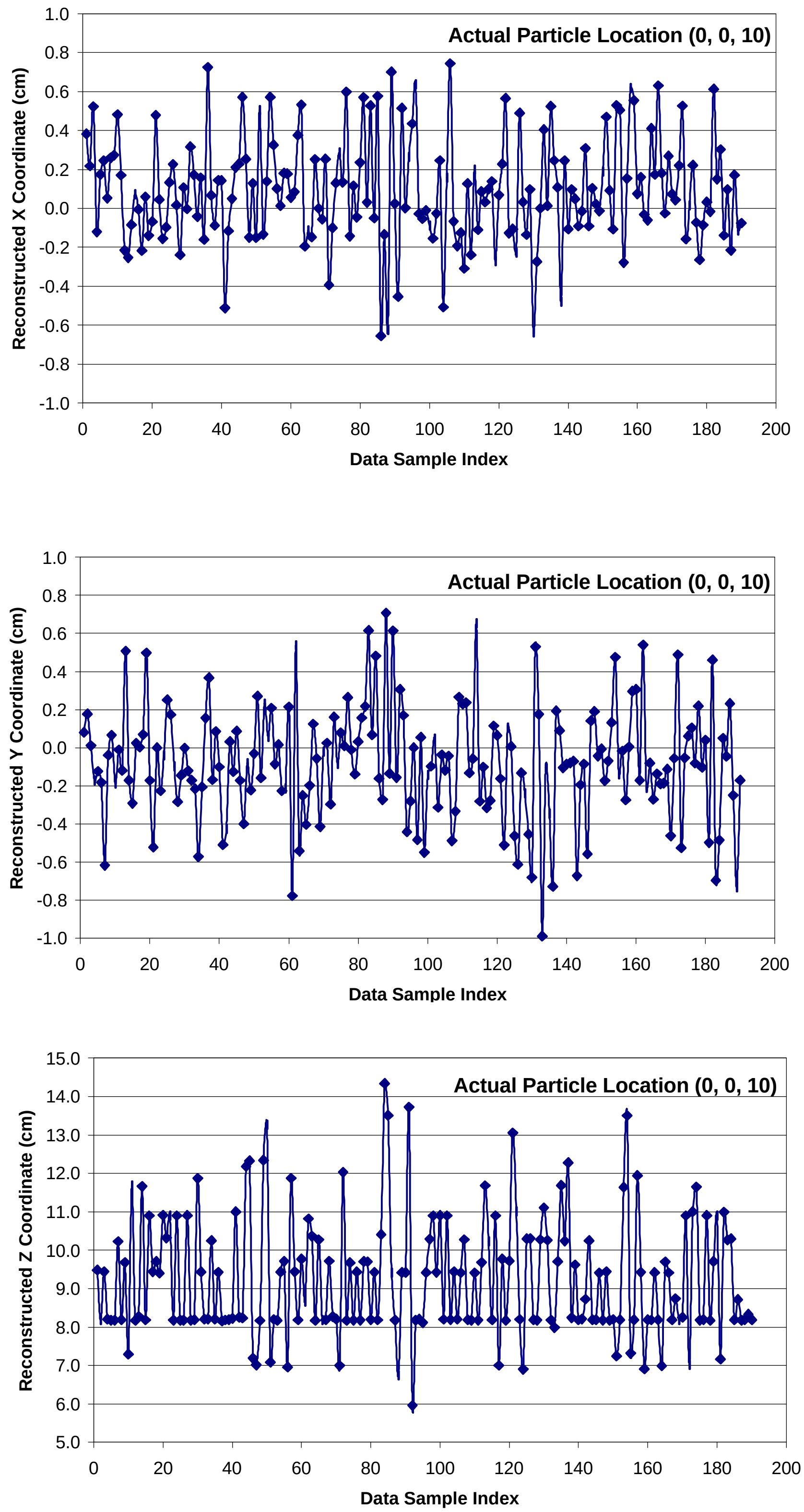

Figure 5.6: Reconstructed Particle Position Over 190 Data Points Acquired Every 20 ms

5.6. Conclusions

The Monte Carlo technique has been validated against experimental data with improved computational efficiency resulting in orders of magnitude reduction in computation times. Further experimentation with more detectors as well as with different data acquisition settings is being carried out to determine the optimal implementation procedure for application to pilot plant scale columns, which are inherently operating with high dispersed phase volume fraction. It should be noted that CARPT is the only technique that can provide information on the velocity fields in large dense opaque systems, where other non-intrusive techniques are entirely inadequate. Hence, our developed Monte Carlo procedure is expected to be used extensively.

5.7. References

Beam, G. B., Wielopolski, L., Gardner, R. P. and Verghese, K., 1978, Monte Carlo calculation of efficiencies of right-circular cylindrical NaI detectors for arbitrarily located point sources, *Nuclear Instruments and Methods*, 154(3), 501-508

Devanathan, N., 1991, Investigation of Liquid Hydrodynamics in Bubble Columns via a Computer Automated Radioactive Particle Tracking (CARPT) Facility, D.Sc. Thesis, Washington University, St. Louis, Missouri

Devanathan, N., Moslemian, D. and Dudukovic, M. P., 1990, Flow Mapping in Bubble Columns Using CARPT, *Chem. Engng. Sci.*, 45, 2285-2291

Dudukovic', M. P., Degaleesan, S., Gupta, P. and Kumar S. B., 1997, Fluid Dynamics in Churn-turbulent bubble columns: Measurements and modeling, American Society of Mechanical Engineers, Fluids Engineering Division (Publication) FED Gas-Liquid Two Phase Flows Proceedings of the 1997 ASME Fluids Engineering Division Summer Meeting, *FEDSM'97*. Part 16 (of 24) Jun 22-26 1997 v 16, Vancouver, Canada

Gupta, P., 1997, Monte Carlo Applications For Multi-Phase Flow Mapping and Visualization Using CARPT, *CREL Annual Report-1997*, 111-126

Larachi, F., Kennedy, G. and Chaouki, J., 1994, A γ-ray detection system for 3-D particle tracking in multiphase reactors, *Nuclear Instruments and Methods in Physics Research A.*, 338, 568-576

Nardi, E., 1970, A note on Monte Carlo calculations in NaI crystals, *Nuclear Instruments and Methods*, 83, 331-332

Saito, K. and Moriuchi, S., 1981, Monte Carlo calculation of accurate response functions for a NaI(Tl) detector for gamma rays, *Nuclear Instruments and Methods*, 185, 299-308

Steyn, J. J., Huang, R. and Harris, D. W., 1973, Monte Carlo calculation of clad NaI(Tl) scintillation crystal response to gamma, *Nuclear Instruments and Methods*, 107, 465-475